ICAS 2016
30th Congress of the International Council of the Aeronautical Sciences
DCC, Daejeon, Korea ; September 25-30, 2016

EXPERIENCE IN AERODYNAMICAL TESTS AND CFD SIMULATIONS OF OVERSIZED WING DEMONSTRATOR IN LARGE LOW-SPEED WIND TUNNEL

Carossa G.M.*, Anisimov K., Chevagin A.**, Efimov R.**, Kursakov I.**, Lysenkov A.**, Malenko V.**, Saprykin A. ****

*** Leonardo S.p.A., Aircraft Division, postal address: Corso Francia, 426, Torino, 10146, Italy, e-mail: giovanni.carossa@leonardocompany.com**

**** Federal State Unitary Enterprise Central Aerohydrodynamic Institute named after Professor N.E. Zhukovsky (TsAGI), postal address: 1, Zhukovsky Street, TsAGI, Zhukovsky, Moscow Region, 140180, Russian Federation**

e-mail: lysenkov@tsagi.ru

Abstract

The subsonic aircraft wing demonstrator is designed and produced by the consortium in the frame of FP7 SARISTU project. To change the morphing wing shape electrical actuators are used. The demonstrator morphing concept is provided by deflection of leading edge (EADN), trailing edge (ATE) and winglet trimmer (WATE). Experimental investigations in the large low-speed wind tunnel (WT) T-104 (TsAGI) with opened test section are carried out in order to demonstrate the wing devices operation.

The numerical simulation of the flow in WT with model installed is carried out in the Reynolds equation system framework with EWT-TsAGI [1] software jointly with the experiment. Computational model created for experimental investigations modeling consists of isolated wing, wing in the WT (Fig. 1), peniche without wing, as well as WT nozzle and diffusor. As a result of calculations additional characteristics are obtained. This allows to estimate an influence of WT flow boundary and experimental setup elements (peniche, sting) on wing integral loads.

The research leading to these results has received funding from the European Union's Seventh Framework Programme for research, technological development and demonstration under grant agreement no 284562.

1 Experimental investigations

Wing demonstrator is installed in the large low-speed WT T-104 (TsAGI) with opened test section. The wing demonstrator is a wing part of 4.7 m length with winglet and with active leading and trailing edges.

The special test rig is designed and produced in TsAGI (Fig. 1) for the wing demonstrator installation in the WT. The experiment consists of two stages: a wing aerodynamics characteristics measurements and the wing systems operation demonstration. Integral wing loads received during first stage then are used for wing strain sensors calibration. Flow parameters in the WT jet are measured at different wing mounting angles.

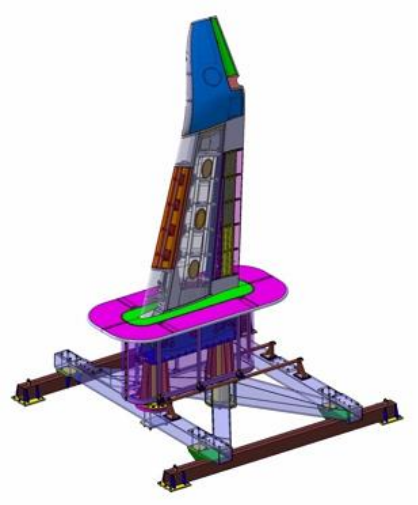

Fig. 1. Test rig overall view

1.1 Model description

The rig for the Wind Demo tests was developed and manufactured by TsAGI. The test rig was mounted on the WT balances cabin (Fig. 2). The Wing Demo root part was connected with the test rig supporting device by a special interface. In order to decrease the bench bottom end influence on the Wing Demo aerodynamics the fairing and the special screen of 1×2.5 m size were used. The screen separated the wind from the supporting device.

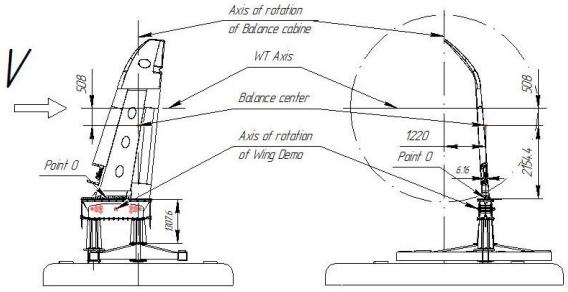

Fig. 2. Scheme of the Wing Demo mounted on WT balances cabin

The fairing was installed on the supporting system lower frame. Thus, the aerodynamic balances were measuring the loads acting not only on the Wing Demo itself, but on the fairing as well. The Wing Demo bottom part was covered with the fairing because the junction unit connecting the wing to the supporting device frame was located lower than the fairing screen.

The Wing Demo size (Fig. 3) was chosen mainly taking into account the following three basic requirements:

- compliance of the Demo structure and internal elements with the real wing;
- compliance with TsAGI's requirements for the models strength tests in the WT;
- compliance with model's requirements for positioning in the WT open test section under the conditions of maximum possible usage of available equipment & instrumentation.

The tests first-priority aim was to check and demonstrate the wing structure functional viability. Thus, the wing scale is increased as much as possible beyond the requirements set for the typical tests in the WTs with the open test section. In this case, as the outcome of the oversized tests bench interaction with the WT flow, the aerodynamic features measurements accuracy reduction might be anticipated.

The Wing Demo AoA was being changed by rotating the balances cabin platform.

Fig. 3. Test rig in T-104

1.2 Experimental results

The main aim of the Wing Demo tests' first stage was the measurements of the aerodynamic loads acting on the wing for in-built strain gages calibration. During the calibration tests the measurements of drag, lift and pitching moment were being done.

Before the Wing loads tests TsAGI performed the preliminary test aimed at the aerodynamic forces definition (L_{ss}, D_{ss}) and ($M_{y\,ss}$), acting on the support system without the Wing. The tests were executed at the flow velocity V=50 m/s. During data processing these loads were subtracted from the balances total readings $L\Sigma$, $D\Sigma$ and $M_{y\Sigma}$:

$L = L\Sigma - L_{ss}$.;

$D = D\Sigma - D_{ss}$;

$M_y = M_{y\,\Sigma} - M_{y\,ss}$

The following configurations were tested:

- wing baseline configuration without morphing devices deflections;
- leading edge deflection configuration;
- trailing edge deflection configuration (deflected at the angle +5° and -5°);
- winglet tab deflection configuration (deflected at the angle +10° and -10°).

Below the dimensionless aerodynamic forces coefficients are used:

$$c_{xa} = \frac{D}{\frac{\rho V^2}{2} \cdot S}, \quad c_{ya} = \frac{L}{\frac{\rho V^2}{2} \cdot S},$$

$$m_{ya} = \frac{M_{ya}}{\frac{\rho V^2}{2} \cdot S \cdot b_a}.$$

The analysis of the graphs (Fig. 4, Fig. 5) shows that the wing has all the typical aerodynamic features, namely the linear character of dependency $C_{ya}=f(\alpha)$. Maximal lift coefficient value at $\alpha=12{,}5°$ is 0.8.

When changing the wing airfoil by deflecting the leading edge, trailing edge and winglet tab, $C_{ya}=f(\alpha)$ inclination line slightly increases and the lift force coefficient rises up to $C_{ya} \approx 0.9$.

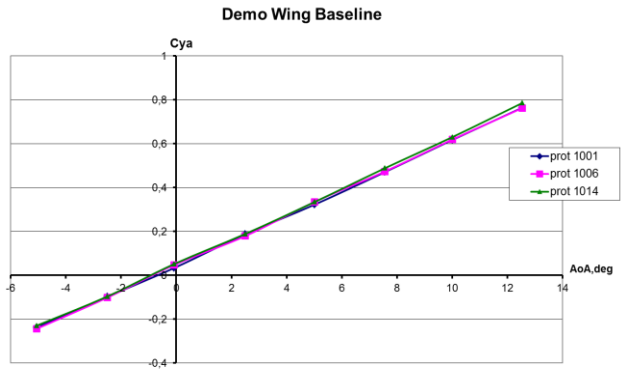

Fig. 4. Lift coefficient

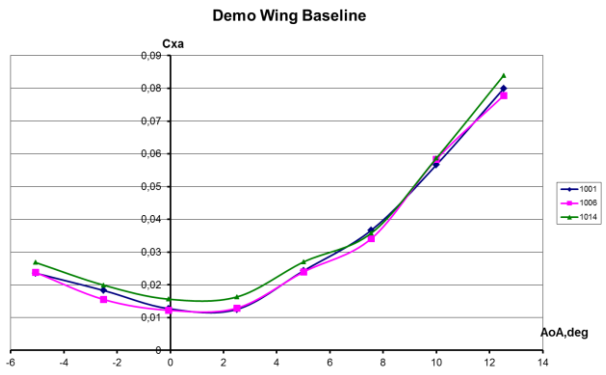

Fig. 5. Drag coefficient

The WT flow features measurements with the rig and wing were executed at velocity V=50 m/s and AoA= 0, 10° after the productive runs completion. The aim of this activity was to estimate the influence of the wing & rig large size on the following factors:

- flow velocity and flow downwash in the WT;
- actual AoA value at the test rig presence in the WT;
- possible change of the flow core boundaries;
- necessity of applying the corrections (and its possible value) to the obtained aerodynamic coefficients.

The experiments were made by using TsAGI's standard methodology. The air pressure six-point sensor was used. The sensor was being moved by a special moving trolley in three directions X, Y, Z. The coordinates initial point was in the center of WT nozzle plane. The pressure measurements were performed in all 6 points of the receiver by the small-sized pressure transducers KDC-24-D-35 and recorded by DAS IVK-M2. Upon the pressure recalculation, TsAGI team defined the dynamic pressures and flow downwash angles in the vertical & horizontal planes in the flow core area in the front of the wing and nearby the flow boundaries (WT shear layer).

The analysis of the obtained data and its comparison with the "empty" WT shows that:

1. The presence of the test rig and the Wing Demo slightly decreases the flow core dimensions compared to the "empty" WT. But more significant transformation can be expected in the lower part of the WT flow due to large rig support frame.

2. The actual dimensionless dynamic pressure coefficient μ is lower than in the "empty" WT.

$$\mu = \frac{(P_0 - p)}{q_\infty}$$

This coefficient goes down to μ = 0.97÷0.98 in front of the wing center & its upper parts (Fig. 6).

The dynamic pressure losses are increased:

- in the wing bottom part, in this area the big thickness of the wing and the test bench supporting device can cause some influence;
- when flow comes nearer to the wing;
- when increasing the AoA.

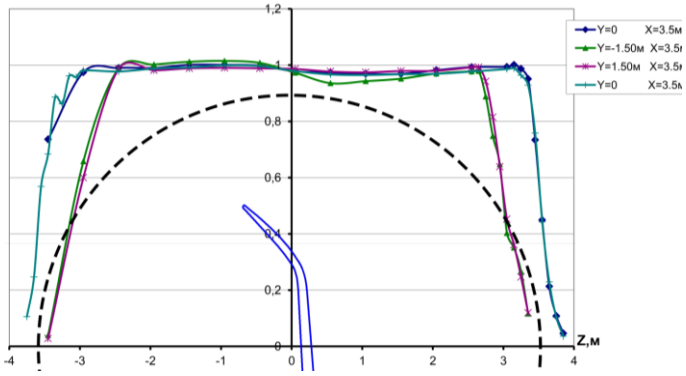

Fig. 6. Distribution of dynamic pressure coefficient μ at AoA= 10°

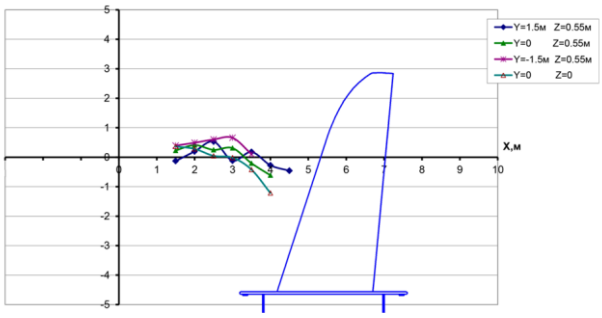

Fig. 7. Distribution of flow downwash angle in the horizontal plane at AoA= 10°.

The difference between the actual coefficient μ from its reference value shows the significant flow deceleration due to the oversized wing and the test rig relative to the WT. Thus, it's reasonable to apply the corrections to aerodynamic coefficients (Fig. 4, Fig. 5) caused by the difference of the real dynamic pressure compared with the theoretical dynamic pressure.

3. The flow local downwash angle in the horizontal plane for the "empty" wind tunnel flow core is not more than 0.3°. When the Wing Demo is present in WT the flow downwash angle tends to increase, especially in front of the wing root part (up to $\beta_{dw} \approx 1.5°$) even at the distance longer than the one chord of the wing (Fig. 7). The flow downwash growth means the wing actual AoA decrease for this value ($\Delta AoA = \beta_{dw}$). The data obtained shows the necessity of inserting the corrections to the aerodynamic moments & forces coefficients.

4.The flow local downwash angle in the vertical plane for the "empty" wind tunnel flow core is not more than $\alpha_{dw} = 0.5°$. When the Wing Demo is present, the flow downwash angle changes slightly in front of the wing center & in its upper part. However, it's likely to increase in the wing root part (up to $\alpha_{dw} \leq 1°$) at the distance longer than the one chord of the wing. Possibly, the vertical flow downwash presence within the mentioned range cannot affect significantly the wing aerodynamic coefficients. Thus, the corrections for these downwashes haven't been further applied.

2 Calculations of wing model «SARISTU» in WT T-104

The methodology and results of simulation of the SARISTU wing with test rig in WT T-104 environment are presented below. All computations were performed by means of in-house code EWT-TsAGI [1]. This software is used in TsAGI for both internal and external aerodynamics tasks. It is used for creating of the mathematical models of wind tunnels (e.g. ETW, Cologne) for detailed in-tunnel simulation.

Goals of investigation:

- to make a visualization of WT test and to present the detailed structure of the flow around experimental facility;
- to estimate the aerodynamic loads;
- to compare them with experimental loads;
- to provide the corrections for test data;
- to estimate the possible reasons of obtained difference of actual and predicted loads.

2.1 Computational method

Program package EWT-TsAGI [1] is used for aerodynamic characteristics calculation. Calculations are carried out in the framework of Navier-Stokes system of equations, closed by SST turbulence model [3], [4]. Second order numerical scheme TVD (GKR) [2] in the form of explicit scheme with implicit smoother is used in the solver. [5]. Structural multiblock computational meshes are used in the solver. The mesh is rebuilt automatically for deferent geometry configurations.

2.2 Mathematical task statement

The geometry corresponds to the real Wing Demo without reflections of its elements. The computations are performed in two formulations with respect of WT (Fig. 8) and without it. In case of in-tunnel computations the basic elements of test rig (WT nozzle and diffusor, test cabin, peniche, additional stand) were taken into account. The computational domain boundaries in general correspond to the WT building walls.

The coordinate system: the X-axis is directed downstream, the Y-axis is directed along the wing span, the Z-axis is oriented to form the right-handed system.

Four variants of test rig configurations are used for computations. They differ in model position with respect to WT nozzle and presence/absence of additional stand of weight cabin (Table 1).

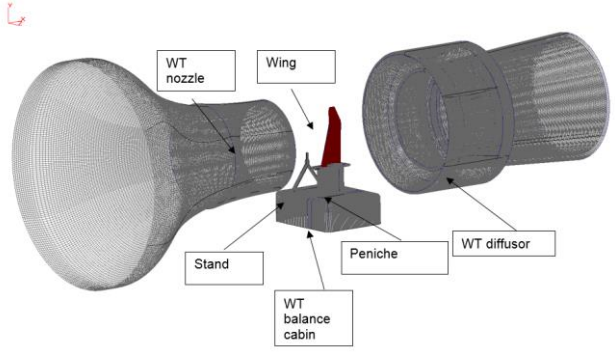

Fig. 8. Computational domain for in-tunnel calculations

Table 1. Computed configurations

Variant №	Distance to WT axis, mm	Stand	Computational mesh, mln cells
1	1220	+	40.5
2	1220	-	38.2
3	520	+	40.5
4	520	-	38.2
5	Free-flight configuration		

2.3 Rig and model position effect on the model characteristics

The in-tunnel simulation is performed with flow parameters as follows: M=0.147 (corresponds to velocity V=50 м/с); incidence and yaw angles $\alpha=0^o$, $\beta=0^o$.

Consider the variation of relative dynamic pressure μ at different Z-coordinate (Fig. 10), with P_0 – local total pressure, p – local static pressure.

$$\mu = \frac{(P_0 - p)}{q_\infty}$$

It can be seen that jet boundaries both in computations and experiment agree with satisfactory level of accuracy. Mach number variation is evaluated by $\Delta M \sim 0.005$. Flow deceleration in the jet center occurs both in computation on experimental results (Fig. 10).

Four variants of rig configuration are considered (Table 1). The results obtained for these configurations indicate that additional left stand of weight cabin which is located in the vicinity of the model as well as the position of the model itself with respect to the jet axis have weak effect on the wing characteristics. This conclusion is confirmed by the distributed characteristics on wing surface (Fig. 10) and flow fields of M and P_0 in the vicinity of the wing (Fig. 11, Fig. 12).

Computations indicate small vortex flow near the peniche (Fig. 13). The estimation done shows that it has no effect on the wing characteristics.

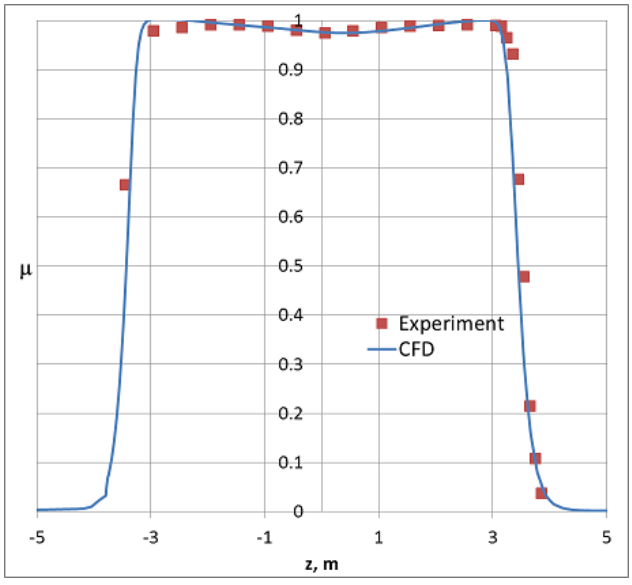

Fig. 9. Distribution of relative dynamic pressure parameter μ along X=3.5m, Y=0m, wing installed, V=50 м/с, α=0

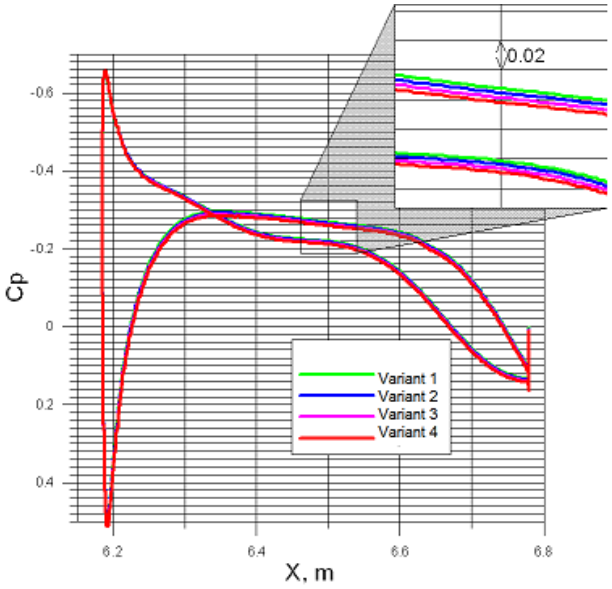

Fig. 10. Cp distribution at section Y=const, V=50 m/s, α=0

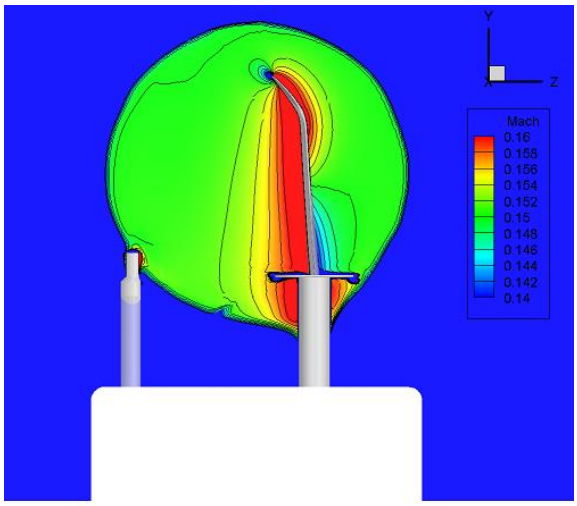

Fig. 11. Variant 1, field of Mach number at section X=const, V=50 m/s, α=0°

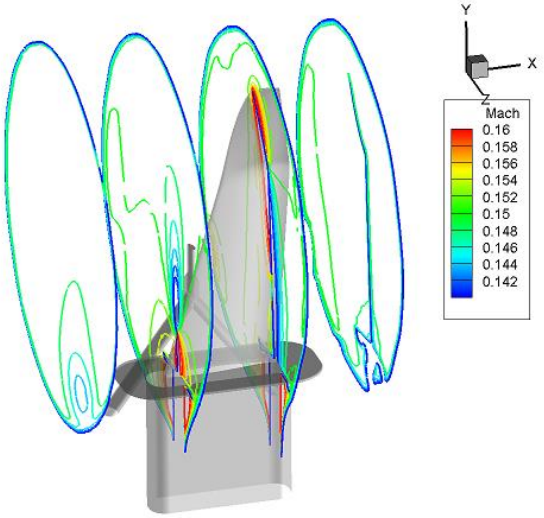

Fig. 12. Variant 1, field of Mach number, V=50 m/s, α=0

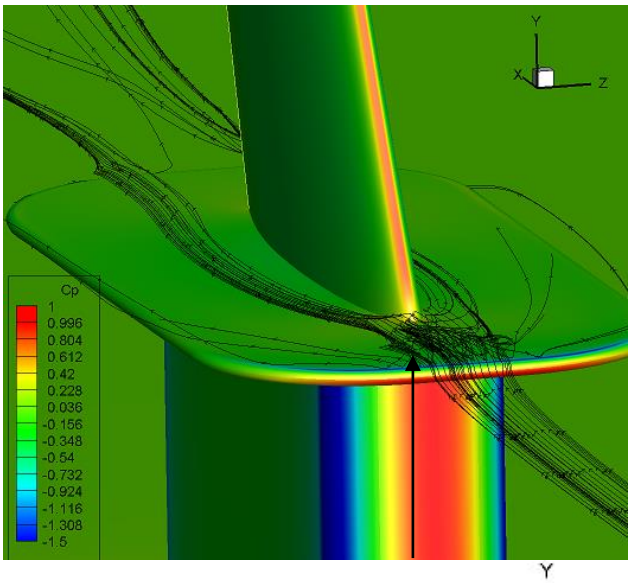

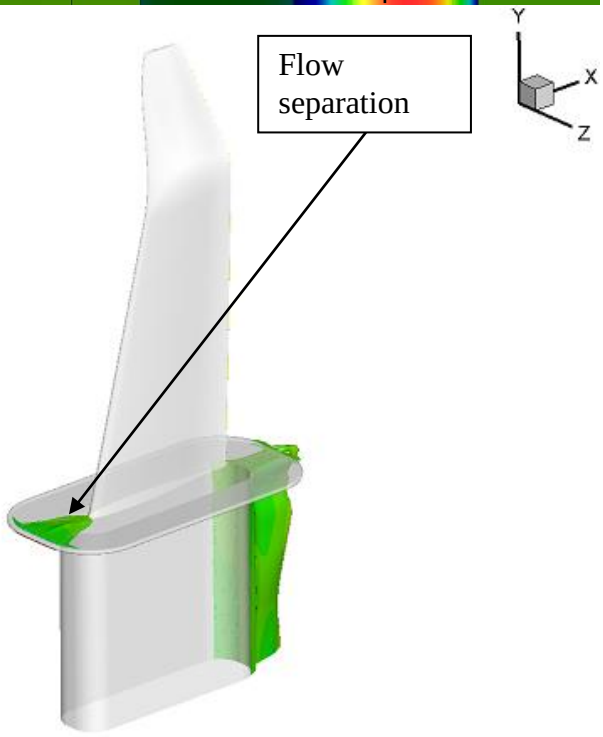

Fig. 13. Flow visualization at the vicinity of peniche, V=50 m/s, α=0

2.4 Estimation of the effects of test conditions on the wing aerodynamics

The comparison between free-flight wing computations and experiment is performed on regime with flow parameters as follows: M=0.147 (V=50 m/c); P_0=102866 Pa; T_0=289.4; α - various; β=0°. Flow parameters used in computations differ from experimental flow characteristics because the simulations are

carried out before the experimental campaign. The results are presented in dimensionless due to this difference. It can be seen that there is a discrepancy between computed (Fig. 14, TsAGI CFD free) and experimental values (Fig. 14, test without corrections) of C_y at α=0 and C_y^{α} (curve slope angle). The reasons of this mismatch are as follows.

1. Flow downwash in empty WT. There is downwash in horizontal plane even in empty WT T-104 of 0.4°. To take it into account this value should be subtracted from the wing installation angle AoA (Fig. 14, test with corrections).

2. Flow downwash due to WT core flow boundaries interference. According results of calculation flow boundaries interference (Fig. 14, TsAGI CFD in WT) leads to substantial transformation of flow near the wing.

It is known [6] that incidence angle correction caused by flow boundaries interference in WT (the same for T-104) could be estimated as:

$$\Delta\alpha_i = \delta_\alpha \frac{S}{F} Cl_{\exp}, \quad (1)$$

with S – wing reference area, F – WT nozzle cross section area, δ_α - interference coefficient.

Values of δ_α for circle jet (flow boundaries in WT T-104) may vary from -0.125 to -0.25. For incidence angle α = 10° the above values of interference coefficients result in diminishing of AoA for $\Delta\alpha$ = 0.74°…1.48°. This is valid in case of moderate blockage of WT. But in our case the test rig and the wing model are oversized and incidence angle correction obtained by (1) is underestimated. For obtaining the appropriate corrections CFD computations could be used.

If assumed that the relation (1) is correct, the values of δ_α could be obtained by comparing the C_y and corresponding α for in-tunnel and free-flight computations (Fig. 14). New δ_α is chosen to match the slope of the blue curve to the red one. This leads to new δ_α = -0.35. For example, for incidence angle α = 10° obtained δ_α results in correction $\Delta\alpha$ = 2.1°.

New correction helps to recalculate experimental data on free-flow condition.

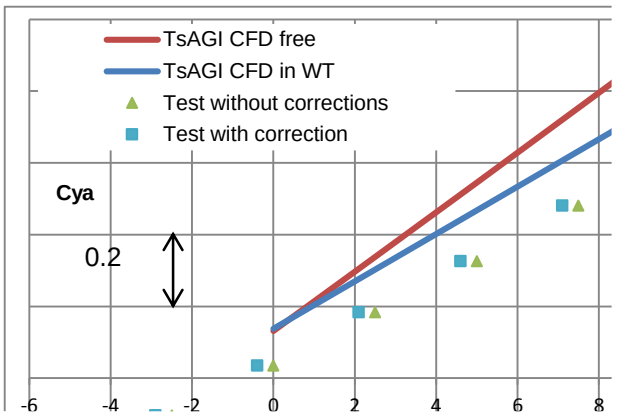

Fig. 14. Comparison of computed and WT test data

4 Conclusion

Within the framework of Grant Agreement №284562 for EU 7FP SARISTU project the full-scale Wing Demonstrator tests were carried out in TsAGI's WT T-104. Computational experiments were carried out with in-tunnel conditions. The results are:

1. Wing Demo balance measurements in T-104 WT were completed for in-built strain gages calibration for flow speed V=30…60 m/s. During the calibration tests the measurements of drag, lift and pitching moment were done.

2. According WT flow features detailed measurements and numerical investigations, a big size of the test rig and essential interference of the Wing Demo with WT core flow boundaries caused to decreasing of an actual angle of attack in comparison with 'free-flight conditions'. Decreasing of actual angle of attack may explain "low" loads obtained in WT.

3. The "Electronic Wind Tunnel" approach were used for calculation of interference coefficient δ_α, needed for re-calculation of actual angle of attack. For example, for incidence angle α = 10° obtained value of δ_α = -0.35 results in correction $\Delta\alpha$ = 2.1°. The obtained corrections of angle of attack are in a good agreement with WT test data received.

References

[1] Neyland, V. Ya., Bosnyakov, S. M., Glazkov, S. A., Ivanov, A. I., Matyash, S. V., Mikhailov, S. V. and Vlasenko, V. V. Conception of electronic wind tunnel and first results of its implementation // *Progress in Aerospace Sciences*, Vol. 37, No. 2, 2001, pp. 121-145.

[2] Toro E.F. Riemann Solvers and Numerical Methods for Fluid Dynamics: A Practical Introduction 2nd Edition, *Springer*, 1999. 645 p. — ISBN: 3540659668.

[3] Menter F.R. Two-equation eddy-viscosity turbulence models for engineering applications". *AIAA-Journal*, Vol. 32, No. 8, 1994. pp. 269 289.

[4] Vieser W., Esch T., Menter F. Heat transfer predictions using advanced two-equation turbulence models. CFX Validation Report. 10/0602, *AEA Technology*. – 2002. Otterfing. Germany, pp. 1 69.

[5] E. V. Kazhan, Stability improvement of Godunov-Kolgan-Rodionov TVD scheme by a local implicit smoother, *TsAGI Science Journal*, Vol.43, 2012, Issue 6.

[6] Pindzola M., Lo C.F. Boundary interference at subsonic speeds in wind tunnels with ventilated walls. // *AEDC*. 1969. No. TR-69-47. pp. 129.

5 Acknowledgment

The Ministry of Education and Science of the Russian Federation financially support part of this work concerning methods of mesh rebuilding. The studies were carried out in the framework agreement №14.628.21.0004 (Project unique identifier RFMEFI62815X0004).

8 Contact Author Email Address

Lysenkov Alexander, PhD, head of group:
tel.: +7 (495) 556-35-16
mailto:lysenkov@tsagi.ru

Copyright Statement